17th World Conference on Earthquake Engineering, 17WCEE
Sendai, Japan - September 27th to October 2nd, 2021

FINITE ELEMENT SIMULATION FOR A LANDSLIDE CAUSED BY THE 2018 HOKKAIDO EASTERN IBURI EARTHQUAKE CONSIDERING THE STRAIN-SOFTENING BEHAVIOR OF CLAYEY LAYER FORMED BY WEATHERING OF PUMICE

N. Kitamura[(1)], N. Bando[(2)], A. Wakai[(3)], T. Soda[(4)], S. Taguchi[(5)]

[(1)] *Graduate student, Department of Environmental Engineering Science, Gunma University, t180c031@gunma-u.ac.jp*
[(2)] *Former graduate student, Department of Environmental Engineering Science, Gunma University, t15303073@gunma-u.ac.jp*
[(3)] *Professor, Department of Environmental Engineering Science, Gunma University, wakai@gunma-u.ac.jp*
[(4)] *Institute of Tephrochronology for Nature and History Co., Ltd., inst-tephra@white.plala.or.jp*
[(5)] *Former undergraduate student, Department of Environmental Engineering Science, Gunma University, t170c042@gunma-u.ac.jp*

Abstract

Natural slopes covered with tephra layers brought from volcanoes are very common in Japan. A landslide caused by the 2018 Hokkaido Eastern Iburi Earthquake was simulated using the finite element method considering the strain-softening behavior of a clayey layer formed by the weathering of pumice. The epicenter of this earthquake was located in the central eastern part of the Iburi region of Hokkaido, and it induced many landslides over a wide area, especially around Atsuma Town. This study investigated a landslide that occurred in the Sakuraoka district of Atsuma Town. The elasto-plastic constitutive model of soils used in the analysis have been proposed by Wakai et al. [1] before. The main purpose of the study is to verify the validity of the numerical method using this model through the simulation of such a recent actual landslide case in Japan.

Based on the results of careful observation of the slope, it was found that the causative material of sliding in the above-mentioned slope was a clay formed by weathered pumice composed the lowest part of "Ta-d" which was erupted from the Tarumae volcano. The material had a high water content and was found to be so sensitive for disturbance. With use of the analytical parameters determined from the results of laboratory tests, a numerical simulation of the landslide was performed by the dynamic elasto-plastic analysis code developed by the authors, where the strain-softening characteristics of the material were appropriately considered by the above constitutive model. In the analysis, the differences in the simulated results with or without consideration of the strain-softening characteristics of the material were examined in particular detail. As a result, it was confirmed that the consideration of them is very important for the accurate simulation of the actual landslide phenomenon such that a shallower soil block in the slope had slipped down a long distance during the earthquake. It was proved that such earthquake-induced landslides can be appropriately simulated by the rigorous analytical method considering all the related mechanical factors such as soil properties, geological structures, topographical conditions and earthquake motion input to the objective slope. The proposed scheme would be applicable for seismic risk assessment of slopes for more general purposes.

Keywords: earthquake, finite element method, strain-softening, landslide, Ta-d

1. Introduction

The 2018 Hokkaido Eastern Iburi Earthquake (Mw 6.7) occurred on September 6, 2018. In the Iburi region, an intensity of 7 on the Japanese seven-stage scale was observed, and it was the highest seismic intensity observed in Hokkaido to date. Many buildings collapsed and slopes failed, causing 41 deaths and 749 injuries and sending 16,000 people to refuges. Landslides occurred over a wide area centering on Atsuma Town in the Yufutsu district. In many of these landslides, a soil block on the slope slipped down a long distance during the earthquake (Fig. 1). As examples of damage over this wide area, the slope collapsed behind a water purifying plant in Tomisato, and sediment flowed down into the buildings [Fig. 2(a)]. In Horosato, soil blocks slid onto a road in spite of originating on a gentle slope [Fig. 2(b)]. In Sakuraoka, a building collapsed and a road was blocked due to a slipped soil block [Fig. 2(c)]. Liquefaction occurred, damaging some roads in Sapporo city, some distance from the epicenter.

The residual deformation of the slope is not always limited to a finite amount of displacement. As described above, sometimes the slope displacement increases extremely. Thus, the damage caused by an

earthquake-induced landslide can generally be classified as either a limited deformation or a catastrophic failure. Because the latter can be much more dangerous, its mechanism should be examined in detail, but creating reliable numerical models of such phenomena has proven to be a challenge. A better understanding of the mechanism of catastrophic slope failures would be helpful for the mitigation of earthquake-related disasters in mountainous districts. A catastrophic failure implies that the slip surface suddenly loses shear strength during an earthquake. If the slip surface can mobilize enough resistance to stop the sliding mass, movement would stop immediately after the earthquake. Whether the sliding mass can be stopped can be simulated by the finite element method.

In this study, the Sakuraoka landslide in Japan, which occurred during the 2018 Hokkaido Eastern Iburi Earthquake was simulated by the finite element method considering the strain-softening behavior of a clayey layer, as previously proposed by Wakai et al. [1]. The purpose of this study was to simulate the slopes that recently failed, and to verify the suitability of the numerical modeling method proposed.

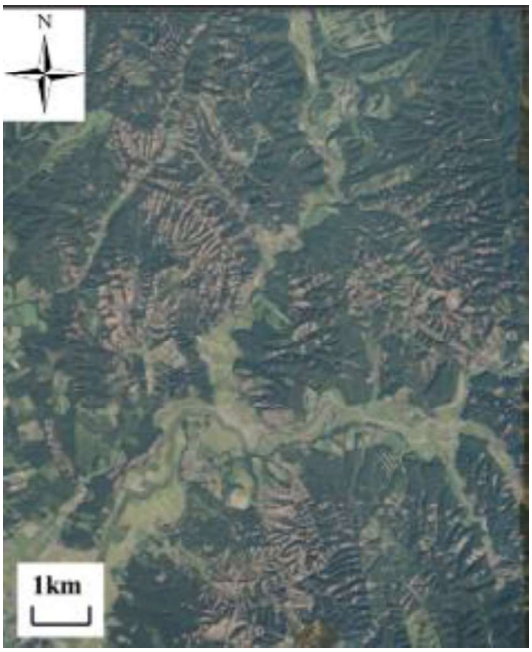

Additions to the map of Geospatial Information Authority of Japan

Fig. 1 Landslides that occurred around Atsuma Town

(a) Landslide in Tomisato

(b) Landslide in Horosato

(c) Landslide in Sakuraoka

Fig. 2 Landslides in Atsuma Town

2. Overview of the Sakuraoka Landslide

Japan has many natural slopes covered with layers of tephra ejected from volcanoes. The geology around Atsuma Town is formed by a clayey layer with such tephra. The Sakuraoka slope examined in this study was a clay formed by a weathered pumice composing the lowest part of the so-called "Ta-d" pyroclastic fall deposit, which originated from the Tarumae volcano. The Sakuraoka landslide was 10 km away from the epicenter, as shown in Fig. 3. The landslide was the failure of a surface block with a length of about 150 m, width of 20-50 m, and depth of about 3 m on an inclination of about 20 degrees. A field survey confirmed that the geology at the landslide site was formed by fallen pyroclastic materials (volcanic ash and andosol) with different depositional ages and degrees of weathering. Furthermore, these deposits are considered to be supported by a largely undisturbed sedimentary structure. The visible geological section was gray to brown weathered pumice prone to slipping (Fig. 4). This layer was confirmed in the location parallel to the slope direction and was thus determined to have been the slip surface. This layer exists at the bottom of the Ta-d pumice fall, which was ejected about 9,000 years ago from the Tarumae volcano. In addition, it was confirmed that the collapsed soil reached the alluvial lowland adjacent to the slope and blocked the road.

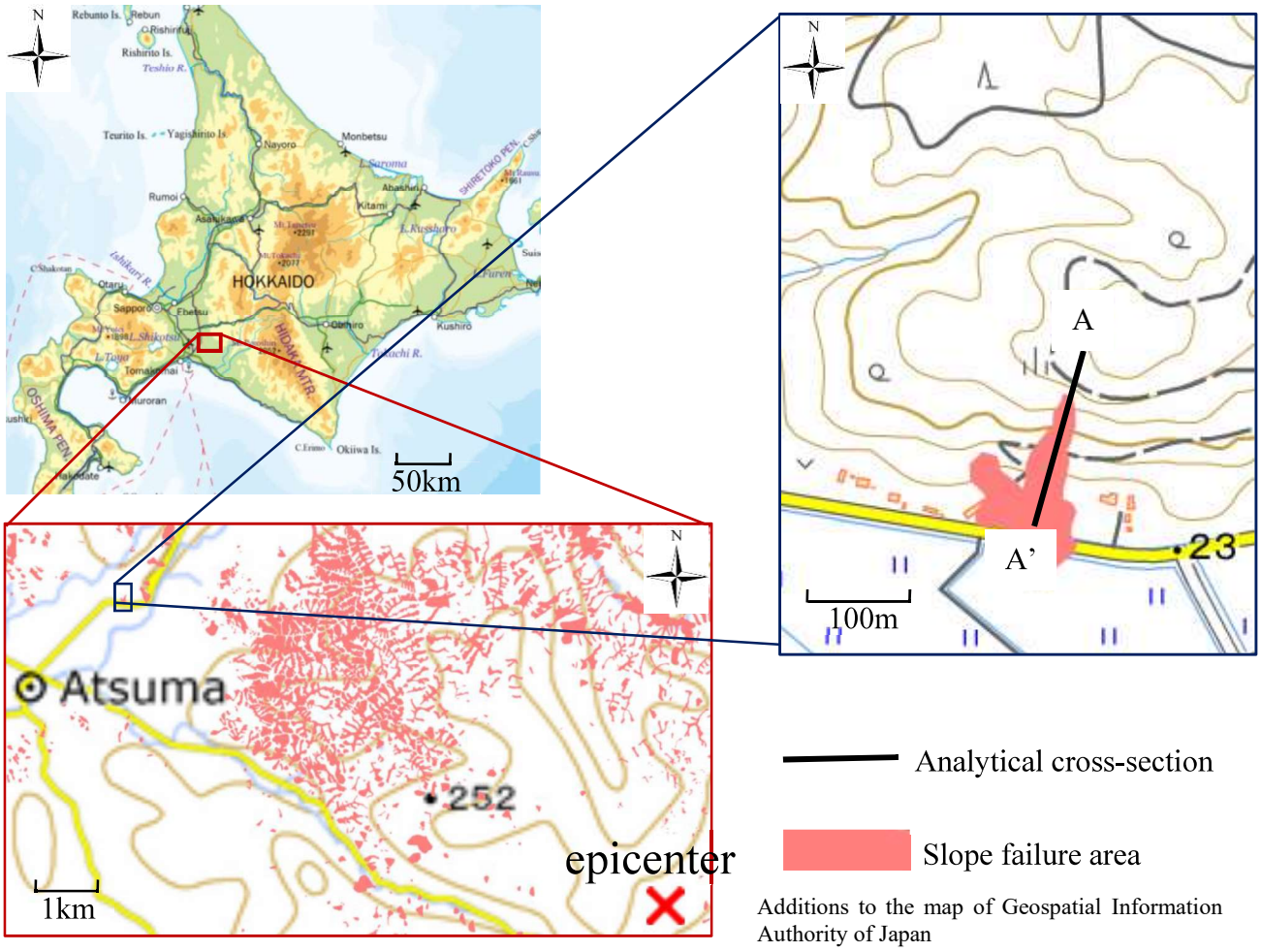

Fig. 3 Location of the Sakuraoka landslide in Atsuma Town

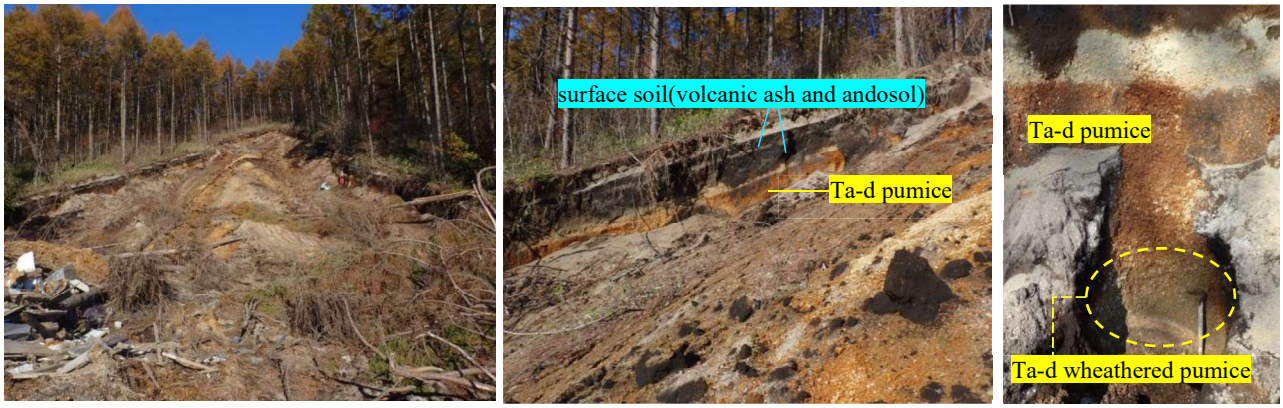

Fig. 4 Overview of the Sakuraoka landslide

3. Analytical Model

To represent the strength degradation of the Ta-d weathered pumice layer induced by an earthquake, it is necessary to analyze the earthquake response with the finite element method. A number of applications for seismic slope stability analysis involving different constitutive models of soil have been reported (e.g., Toki et al. [2], Griffiths et al. [3], Ugai et al. [4]). However, because these models possess a large number of independent parameters, it may be difficult to adequately determine all of the necessary input parameters. Thus, a simple constitutive model with high prediction accuracy is needed for this problem. In this regard, Wakai and Ugai [5] proposed a moderately simple constitutive model that is based on the dynamic deformation characteristics and shear strength of the soil. In addition, it has been proposed that strain-softening phenomena be taken into account with this model (Wakai et al. [1]).

3.1 Material Composition

The UW softening model [1] was adopted for the constitutive law of the Ta-d weathered pumice layer, which is considered to have exhibited cyclic softening behavior, while the UW model [5] without considering softening properties was adopted for each of the other materials. Detailed explanations are given in the cited references. In the UW softening model, the shear strength, which gradually decreases as plasticity increases during an earthquake, is given as follows:

$$\tau_f = \tau_{f0} + \frac{\tau_{fr} - \tau_{f0}}{A + \gamma^p}\gamma^p, \tag{1}$$

where τ_{fr} is the residual shear strength after large shear deformation, which is usually much smaller than the initial shear strength τ_{f0}; γ^p is the accumulated absolute value of plastic shear strain; and A corresponds to the magnitude of γ^p accumulated at the point where the shear strength drops to a value of mean of τ_{f0} and τ_{fr}. When these parameters are determined with a direct shear test, they need to be converted to shear strain values that assume, for convenience, that the inside of the shear box is under a uniform simple shear.

3.2 Finite Element Modeling for Dynamic Response Analysis

To simulate the earthquake-induced landslide behavior at Sakuraoka, a finite element model for a two-dimensional cross-section of the target slope (Fig. 3) along the sliding direction was created (Fig. 5). This model was developed based on the findings of the field survey described in Section 2. The mountain (uphill) side of the slope has a gradual decrease in elevation. The average thickness of each layer in the analytical cross section is given in Table 1. The finite element meshes is composed of eight-node elements, which are quadratic elements suitable for higher-order deformation with nodes at the midpoints of each side of the apparent grid

used for the simulation. The displacement history at Point A in Fig. 5 was shown in detail. The boundary conditions were fixed both horizontally and vertically at the lower end, and fixed horizontally at the left and right ends of the figure, which is a standard condition in dynamic analysis. To avoid the influence of reflected waves at the left and right ends, buffer regions were provided on both sides to increase the distance between the left and right ends and the main part of the analysis target. Seismic waves were input as horizontal acceleration components from the bottom of the finite element meshes.

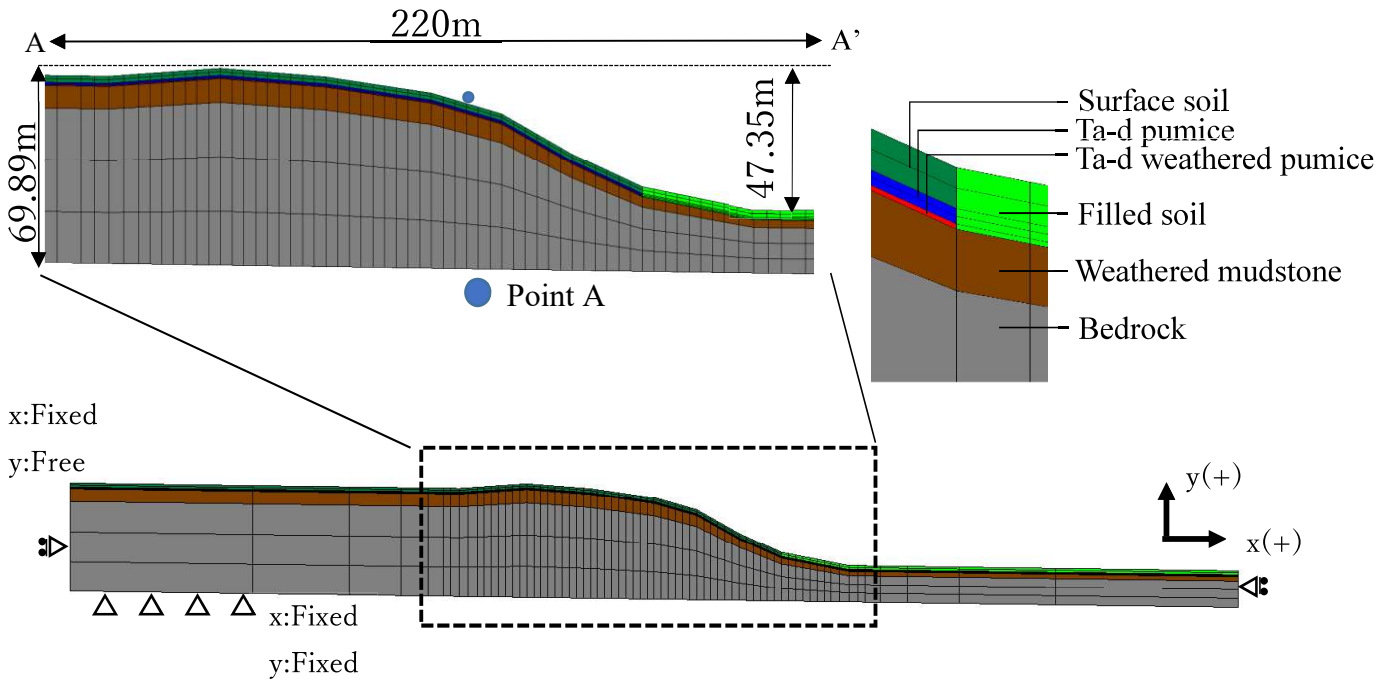

Fig. 5 Finite element meshes used for the numerical simulation at cross section A-A'

Table 1 Average thickness of layers

Layer's name	Average thickness of layers[m]
Surface soil	2.4
Filled soil	3.6
Ta-d pumice	0.9
Ta-d weathered pumice	0.3
Weathered mudstone	5.7
Bedrock	38.3

Conventional finite element procedures were used to discretize the equation of motion of the global system as

$$[M]\{\ddot{u}\} + [C]\{\dot{u}\} + \{P\} = -[M]\{\ddot{U}\} \tag{2}$$

where $\{P\}$ is a nodal force vector that is equivalent to the total stress acting inside each element. If the system behaves as an elastic body, then $\{P\} = [K]\{u\}$. In addition, $[M]$, $[U]$, and $[K]$ are the mass, damping, and stiffness matrices, respectively, and $\{u\}$ and $\{U\}$ are the relative displacement vector at each node and the absolute displacement vector at the base, respectively. Newmark's β method is used to integrate Eq. (2) with respect to time. The effect of viscous damping based on Rayleigh damping is adopted as

$$[C] = \alpha[M] + \beta[K] \tag{3}$$

The parameters for Rayleigh damping ($\alpha = 0.172, \beta = 0.00174$) were chosen so that h due to viscous damping is temporarily maintained at approximately 3%.

3.3 Material Parameters for the Simulation

To simulate soil failure, it is very important to provide appropriate parameters. The parameters used here are shown in Table 2. The parameters of the Ta-d weathered pumice layer were determined based on laboratory test results. Young's modulus was estimated mainly from the N-values of borehole survey data near the target area. For the other parameters, general values, such as those of the example values introduced in the reference [6], were used. The hysteretic damping parameters $b \cdot \gamma_{G0}$ and n are the constants that govern the hysteretic damping used in the UW model. These parameters for each layer were determined with reference to the past literature [7]. With these hysteretic damping parameters, the UW softening model was used to simulate the hysteretic loop of the cyclic loading, as shown in the Fig. 6. The shear strength tends to significantly decrease under cyclic loading by seismic motion. In this study, the difference in the results between the cases with and without strain-softening is considered. For this purpose, Case 1 is with strain-softening and Case 2 is without strain-softening.

Table 2 Material parameters used in the finite element simulation for the Sakuraoka landslide

Materials	Surface soil	Filled soil	Ta-d			Weathered mudstone	Bedrock
			pumice	weathered pumice			
				case1	case2		
Young's modulus E(kN/m^2)	45000	45000	25000	25000		400000	1000000
Poisson's ratio ν	0.4	0.4	0.4	0.45		0.3	0.2
Cohesion c(kN/m^2)	5	15	25	25		4000	10000
Internal friction angle Φ(deg)	35	30	25	21		30	40
b・γ_{G0}(Parameter for damping)	2.06	5.15	7.29	9.50		5.50	6.20
n(Parameter for damping)	1.60	1.53	1.42	1.2		1.01	1.05
Unit weight γ(kN/m^3)	16	16	14.5	14.5		20	25
Residual strength ratio τ_{fr}/τ_{f0}	-	-	-	0.01	-	-	-
A (Parameter for softening)	-	-	-	0.11	-	-	-

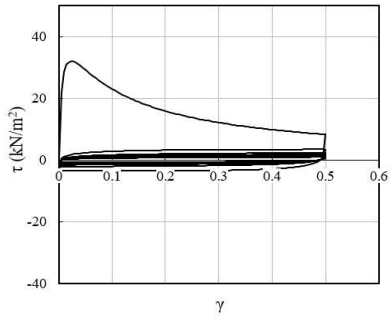

Fig. 6 Simulated hysteretic loops with use of the UW softening model

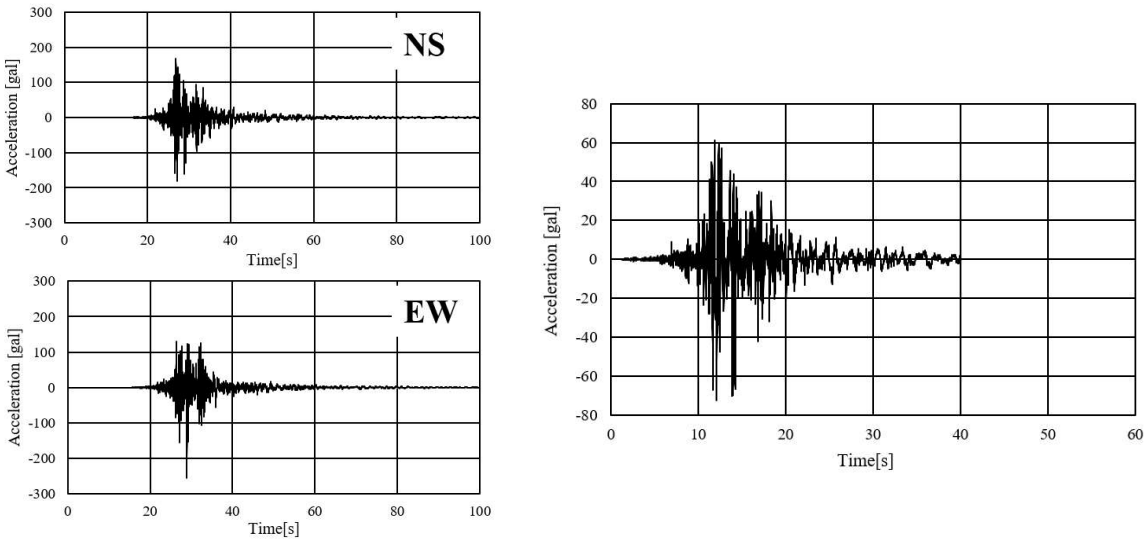

Fig. 7 Observed bedrock acceleration record at the KiK-net Oiwake station (left) and input motion applied at the bottom of the finite element meshes (right)

3.4 Input the Seismic Motion

The seismic waves used in the analysis are based on the bedrock waveforms observed at the Oiwake station of KiK-net, the strong motion observation network of the National Research Institute for Earth Science and Disaster Resilience of Japan. The Oiwake station is located 16.5 km away from the Sakuraoka landslide. The left side of Fig. 7 shows the EW and NS components observed at the Oiwake station. The waveforms were corrected to align with the direction of the analysis area, and the distance attenuation equation of Si and Midorikawa [8] was used to take into account the distance between Sakuraoka and the Oiwake station. After that, bedrock waves in the target slope were estimated with an inverse analysis. For this purpose, microSHAKE (Jishin Kogaku Kenkyusyo, Inc.) was used. The seismic waveforms used in the above analysis are shown in the right side of Fig. 7.

4. Analytical results

Fig. 8 and Fig. 9 show the residual deformations and residual shear strain distributions, respectively, with and without softening. In Fig. 8, the black dotted lines represent the ground before the earthquake and the red line represents the ground after the earthquake. The results of Case 2 without strain-softening did not show as large deformation as Case 1. In Fig. 9, the increasing strain is shown with shades of gray, with black indicating the highest strain. In Case 1, large strains occurred in the Ta-d weathered pumice layer. In contrast, in Case 2,

there had fewer strain areas of the Ta-d weathered pumice layer than Case 1. From the above results, it can be concluded that the landslide mechanism is more similar to that of Case 1 with strain-softening.

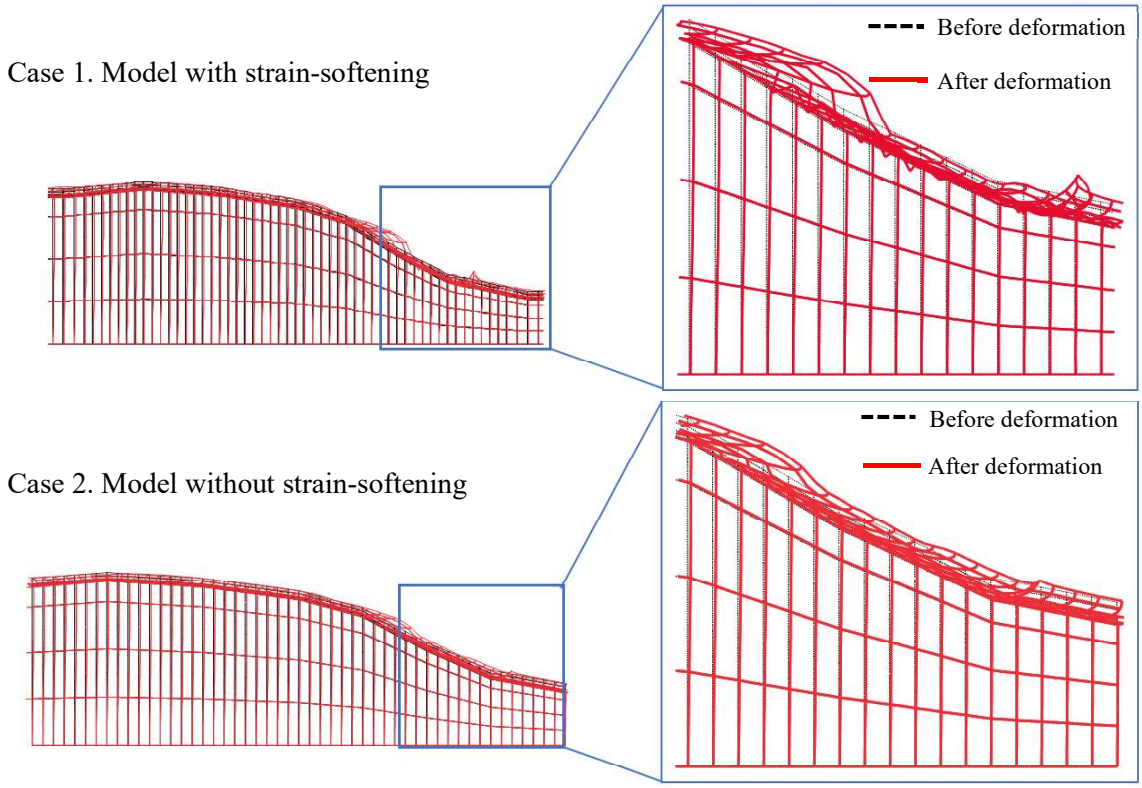

Fig. 8 Calculated residual deformations at the end of analysis (50s passed) with and without consideration of strain-softening

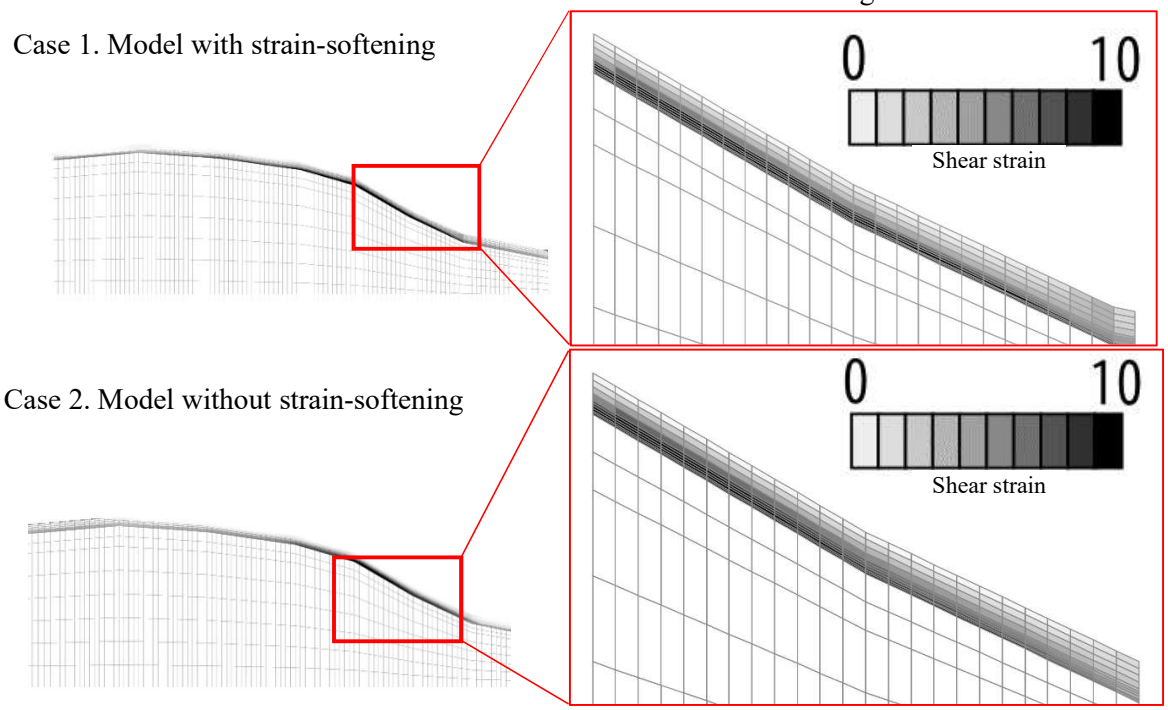

Fig. 9 Calculated residual shear strain distributions with and without consideration of strain-softening

The time histories of the horizontal displacements in Case 1 and Case 2 calculated at Point A (Fig. 5) are shown in Fig. 10. In Case 1, both displacements started to increase around 3 seconds, and the displacements continued to increase during the excitation. Conversely, in Case 2, the displacements increased during the shaking, but remained constant after 40 seconds, when the shaking stopped. This result suggests that in Case 1 with strain-softening, the displacement continued to increase due to the stress concentration caused by the strength reduction (strain-softening) at the sliding surface, which could not support the soil mass above it. In Case 2 without strain-softening, it is thought that the resistance to sliding of the soil mass was maintained and deformation was suppressed.

Accordingly, a catastrophic failure can be evaluated as the balance between $\sum R_f$ and $\sum T_s$, where $\sum R_f$ is the total shear strength along the slip surface and $\sum T_s$ is the weight of the upper sliding mass. The following index F_d is introduced to predict catastrophic failure [1]:

$$F_d = \frac{\sum R_f}{\sum T_s}. \tag{2}$$

Fig. 11 shows the time histories of the stability index F_d for each case. In Case 1, F_d becomes 1.0 at the moment when the displacement starts to increase compared to the horizontal displacement in Fig. 10. Conversely, in Case 2, the shear strength of the slip surface is not lost due to repeated loading during the earthquake, and F_d becomes a constant value. When the F_d drops below 1.0, the shear resistance on the slip surface is no longer sufficient to hold back the self-weight sliding force of the soil mass on the slip surface, and continuous activity begins. The change of F_d in Case 1 is consistent with the actual landslide mechanism. This index was found to be useful in explaining the catastrophic failure.

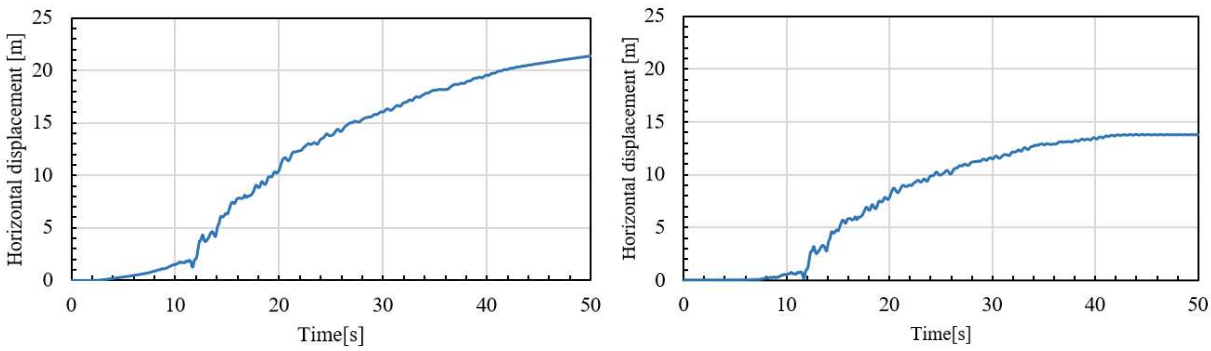

Case 1 (Consideration of strain-softening) Case 2 (Without consideration of strain-softening)

Fig. 10 Calculated time histories of horizontal displacement at Point A with and without consideration of strain-softening

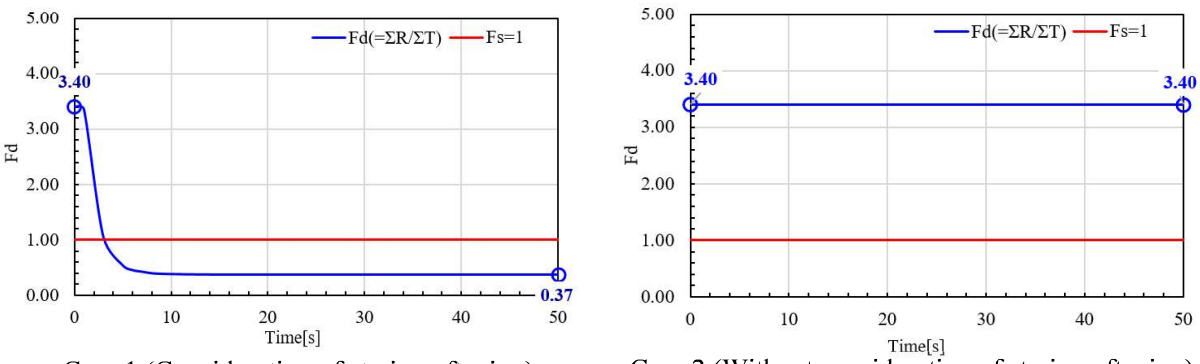

Case 1 (Consideration of strain-softening) Case 2 (Without consideration of strain-softening)

Fig. 11 Time histories of the stability index F_d

Finally, Fig. 12 shows the distributions of the shear strength τ_f and mobilized shear stress τ along the slip surface at each time step in Case 1 and Case 2. Those values have been calculated as the average of Gaussian point values in each element. The horizontal distance x is the distance from the left side of the targeted area, as shown in the right graphic in Fig. 12. As shown in the figure, before the earthquake, the upper sliding block was safely supported by the shear resistance along the slip surface in both Case 1 and Case 2. The stress was concentrated at the toe. In Case 1, the shear strength τ_f gradually decreased during the earthquake due to strain-softening of the Ta-d weathered pumice layer. In Case 2, the shear strength τ_f remained constant during the earthquake, but the mobilized shear stress τ fluctuated. The shear stress at the end of the earthquake was similar to the initial condition. These results support the validity of the concept of catastrophic failure based on Fig. 11.

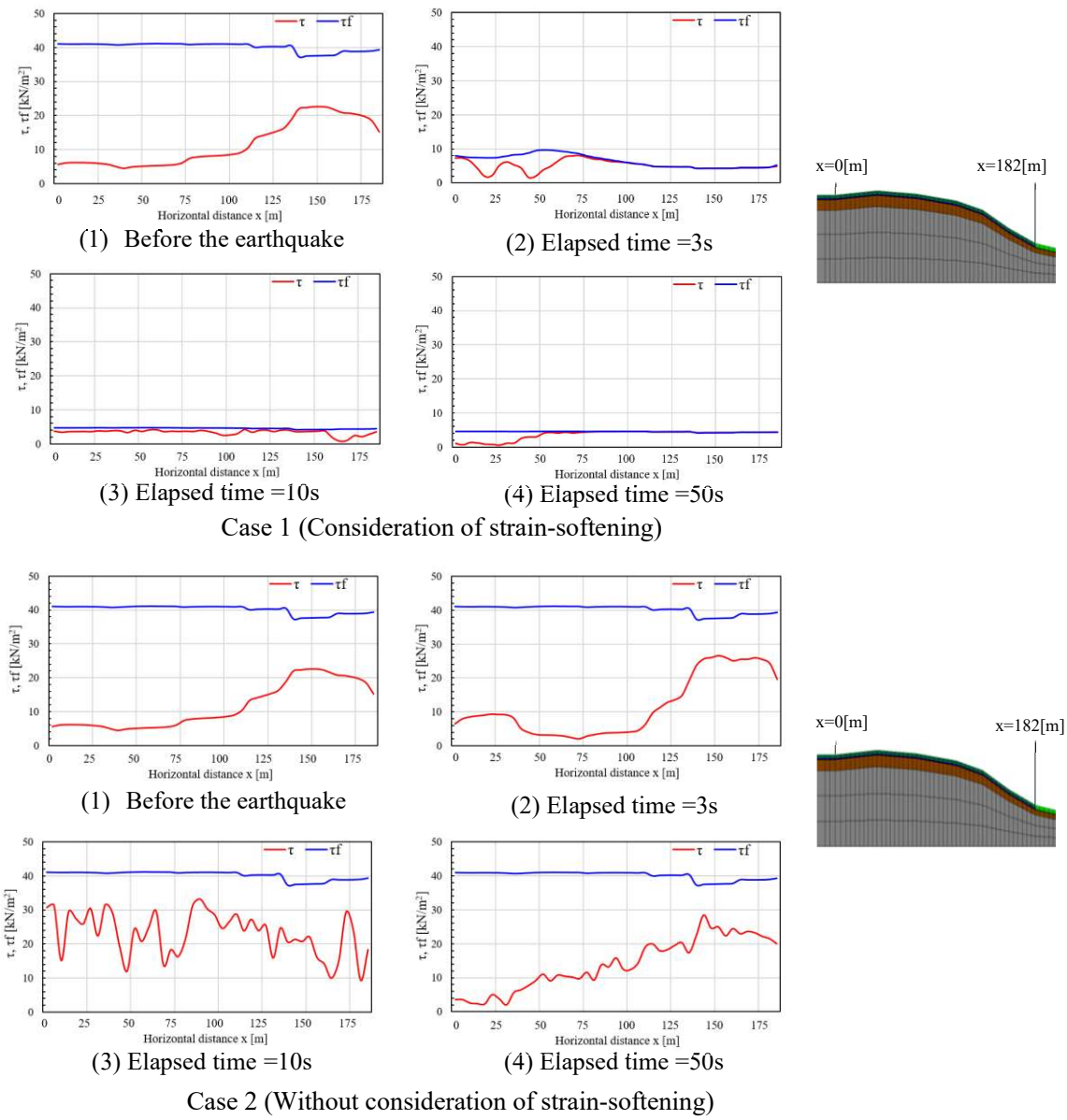

(1) Before the earthquake
(2) Elapsed time =3s
(3) Elapsed time =10s
(4) Elapsed time =50s
Case 1 (Consideration of strain-softening)

(1) Before the earthquake
(2) Elapsed time =3s
(3) Elapsed time =10s
(4) Elapsed time =50s
Case 2 (Without consideration of strain-softening)

Fig. 12 Distributions of $\boldsymbol{\tau_f}$ and mobilized shear stress $\boldsymbol{\tau}$ along slip surface

5. Conclusions

The main findings of this study are summarized as follows.

(1) The slope collapse in the Sakuraoka district, Atsuma Town, which occurred during the 2018 Hokkaido Eastern Iburi Earthquake, was simulated using a two-dimensional dynamic elasto-plastic finite element method. By adopting the UW softening model [1], which can account for the strain-softening of soil due to cyclic loading, the slope failure phenomena during the earthquake were accurately simulated.

(2) The results of deformation diagrams and strain distribution diagrams with and without strain-softening showed that the results with strain-softening were closer to the actual landslide, suggesting the usefulness of considering strain-softening.

(3) When strain-softening of the sliding surface is taken into account, the stability index F_d is the ratio of the maximum shear resistance force $\sum R_f$ on the sliding surface to the sliding force $\sum T_s$ on the sliding surface due to the self-weight of the sliding soil mass. Slope failure is considered to occur when this ratio falls below 1.0.

The results of this study will be useful for evaluating the seismic hazard of slopes with geological structure and geological age similar to that of the slope examined in this study.

6. Acknowledgements

We are grateful to Prof. Kotaro Yamagata at the Joetsu University of Education for his assistance in the field survey of the tephra layers.

7. References

[1] Wakai A. ,Ugai K. ,Onoue A. ,Kuroda S. and Higuchi K.(2010): Numerical Modeling of an earthquake-induced landslide considering the strain-softening characteristics at the bedding plane, Soils and Foundations, Vol.50, No.4, pp.515-527.

[2] Toki K. ,Murata F. and Oguni Y. (1985): Dynamic slope stability analyses with a non-liner finite element method, Earthquake Engineering and Structural Dynamics, Vol. 13, pp. 151-171.

[3] Griffiths D. V. and Prevost, J. N. (1988): Two-and three-dimensional dynamic element analyses of the Long Valley Dam, Geotechnique, Vol. 38, No. 3, pp. 367-388.

[4] Ugai K. , Wakai A. and Ida H. (1996): Static and dynamic analyses of slopes by the 3-D elaasto-plastic FEM, Proc. Of 7th International Symposium on Landslides, pp. 1413-1416.

[5] Wakai A. and Ugai K. (2004): A simple constitutive model for the seismic analysis of slopes and its applications, Soils and foundations, Vol. 44, No. 4, pp. 83-97.

[6] Japanese Geotechnical Society (2003): Understanding the elasto-plastic finite element method - FEM series for geotechnical engineers ②, pp. 193-209 (in Japanese).

[7] Ishihara K. (1976): Fundamentals of soil Dynamics, Kajima Institute Publishing Co., Ltd., p196(in Japanese).

[8] Si H. and Midorikawa S. (1999): New attenuation relationships for peak ground acceleration and velocity considering effects of fault type and site condition, J. Struct. Constr. Eng., pp. 63-70 (in Japanese).

